PROCEEDINGS OF SCIENCE

A Preliminary Look at the Construction of the 4HWC Very High and Ultra High Energy Source Catalog Using the Multi Source Fit Method

Samuel Groetsch[a,*] **for the HAWC collaboration**

[a] *Michigan Technological University,*
1400 Townsend Dr, Houghton MI, United States

E-mail: sjgroets@mtu.edu

The High Altitude Water Cherenkov (HAWC) observatory is highly suitable for large-scale survey work. The high duty time (95%), large instantaneous FoV (2 sr), and sensitivity over the 300 GeV to more than 100 TeV energy range make it ideal for creating a catalog of very high energy (VHE) sources. Over the lifetime of the HAWC observatory, 4 catalogs have been produced 3 of which were constructed utilizing the full HAWC energy range while another used a restricted (>56 TeV) range. This talk will focus on the status of the planned 4HWC (full energy range) catalog including the newly developed Multi-Source Fit algorithm inspired by the Fermi Extended Source search method for the galactic plane. Using at least an additional 1000 days of data, improved event reconstruction algorithms using HAWC's newly completed fifth pass through its dataset, and the improved search algorithm we expect to see a major improvement in the sensitivity and accuracy compared to previous catalogs. Additionally, this talk will present preliminary results from tests of the algorithm in "Benchmark" regions in HAWC data, including but not limited to, the Crab Nebula and The Cygnus Cocoon

38th International Cosmic Ray Conference (ICRC2023)
26 July - 3 August, 2023
Nagoya, Japan

*Speaker

PoS(ICRC2023)759

1. The Multi-Source Fit Algorithm

The newest improvement to the HAWC γ-ray catalog is an adaptation and extension of methods used in other source catalogs such as the Fermi Galactic Extended Source Catalog[1] and 1HWC catalogs. While the logical structure of the Multi-Source Fit (MSF) method is based on the Fermi Extended Source Method used in the Fermi Galactic Extended Source Catalog this implementation is greatly expanded to perform a blind point source search of the γ-ray data in HAWC and perform both an "Extension" and "Curvature" test. I will go through each subsection of the MSF algorithm in the order it is run. The subsections are Point Source Search, Extension Test and Distance Cut, Curvature Test, and a Final Refit.

1.1 Point Source Search

The point source (PS) search begins by looking at the generated significance map made by the putative PS search [2] common to nearly all significance maps seen from the HAWC observatory. Depending on the galactic latitude of the center of the region of interest (ROI) that the method is using we first add a simple Diffuse Background Emission (DBE) Model which consists of an elongated Gaussian emission model in the direction of the galactic plane that extends $\pm 1^\circ$ in latitude. The DBE model has a fixed morphology and spectral index ($\Gamma = -2.75$) based on a simple power law. The Flux normalization is fit and the fit moves onto adding PSs with a simple power law assumption.

$$SimplePowerLaw = N_0 \left(\frac{E}{E_0}\right)^{-\Gamma}$$

If the ROI is far away from the plane (>10°) no DBE model is added and instead we immediately move to the PS adding phase. The PS adding begins by finding the pixel with the largest significance in the map and using the pixel's location as the initial guess for the PS model. After the maximum likelihood model is found with the added PS we create a residual map by subtracting the model map from the data map and we find the new most significant pixel in this residual map which serves as the guess for a new PS model. Before moving to add the next PS model we freeze the location parameters for the PS model fit during this step. After the first point source is added and the location frozen we create a test statistic (TS)

$$TS = 2 \cdot \log \frac{L_{FitModel}}{L_{Background}}$$

where the Fit Model is the result from the current model and background is the result from the previous fit model. For example, when adding the 4th PS we will compare the ratio of the likelihood of the 4 PS model and the 3 PS model to create this test statistic. From Wilks' Theorem [3] this test statistic will be distributed as a χ^2 with degrees of freedom (DoF) equal to the number of additional parameters. For the PS adding phase, we have 4 new parameters for each additional PS model so we use a threshold of a minimum of 25 TS to accept the new PS model into our model of the region. This roughly corresponds to a significance threshold of 3.9 sigma due to the number of DoF. Once the PS adding phase terminates based on the TS threshold we will move on to the Extension Test portion of the MSF algorithm.

1.2 Extension Test and Distance Cut

For each PS model, we now will test to see if an extended Symmetric Gaussian with an extension parameter will fit the data better. For each model, we find a source TS by holding the other sources fixed and treating them as the background model. Then beginning with the source with the highest source TS we substitute the PS model with the extended model and fit the location, extension, and spectral parameters of the newly extended source while also allowing the spectral parameters of the other sources in the model to be fit. This results in one additional parameter in total and as such the square root of the TS corresponds to the significance level. So to maintain a consistent significance threshold between the PS adding phase and the alternate model hypothesis we set the TS threshold at 16 to accept the extended model over the simpler PS model. If the extended source assumption is accepted we then again evaluate the source TS of all the source models in the model and remove any sources which fall below the 25 TS threshold. If a source is dropped within 0.5° of another source that remains in the model we refit the model with the location and morphology (in the case of extended source models) of any sources near the dropped sources free. This may iterate several times if the morphology changes drastically between refits. Once the model is stable and no sources are dropped we move on to the next most significant source remaining in the model. For most regions, many of the PS models added in the PS adding phase will not "survive" the extension test phase and a much more simple (in terms of the number of parameters) model of the region that still explains much of the emission moves on. After the Extension Test is performed on all sources in the model a final "cut" based on the minimum distance (0.3°) between sources is applied to remove possible aberrations in the data near extremely bright sources like the Crab Nebula. So far this cut has only influenced the Crab Nebula region and is not expected to influence any other regions tested. Once the distance cut is finished we move on to the spectral curvature test.

1.3 Curvature Test

Once the simplified model of the region using PS and Extended models is finished we then test if a curved spectral assumption is more favored for each source. In the exact same way as the Extension Test, we test each source moving from most significant to least significant and substitute the simple power law assumption with a log parabola spectral assumption. The addition of the beta parameter allows for the spectrum to curve downwards at higher energies as we expect the higher energy emission to have a softer spectrum for sources especially pulsars and pulsar wind nebulae.

$$SimplePowerLaw = N_0 \left(\frac{E}{E_0}\right)^{-\Gamma}$$

$$LogParabola = N_0 \left(\frac{E}{E_0}\right)^{-\alpha+\beta \log\left(\frac{E}{E_0}\right)}$$

1.4 Final Refit

The final step of the MSF algorithm is aptly named the final refit and consists of freeing all the location, morphology, and spectral parameters of the models still remaining in the best-fit model and doing a final fit. This allows for sources that may not have been accepted as Extended, Curved, or otherwise had their location freed throughout the fitting process to "settle" into their true best fit.

This also allows extended sources that were chosen early on in the process to adapt to any major changes that occurred close enough to influence their best-fit location but did not trigger a refit for any number of reasons. This step is crucial in highly complex regions and also assists in getting the best source TS calculations for when the full source list will be compiled.

2. Regions Tested

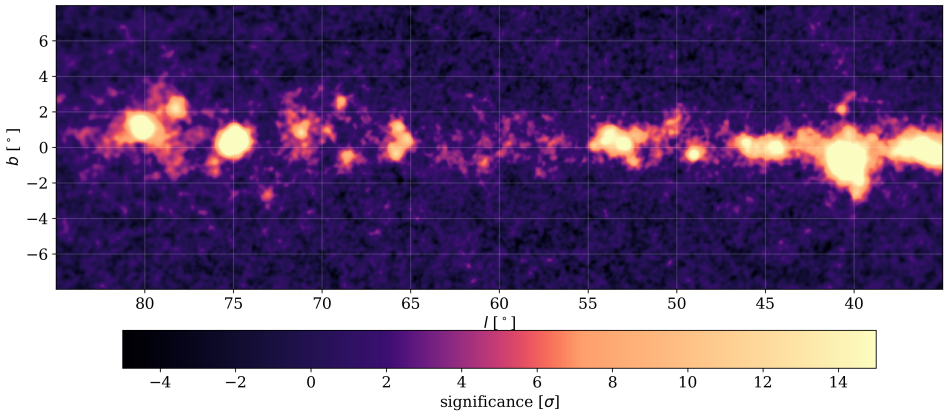

Figure 1: View of a portion of the galactic plane in HAWC data from 35° to 85° and ±7.5° off the plane

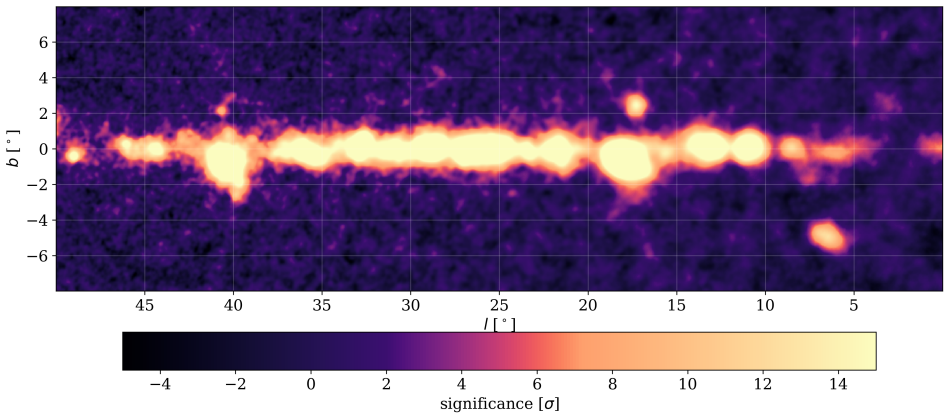

Figure 2: View of a portion of the galactic plane in HAWC data from 0° to 50° and ±7.5° off the plane

Two regions will be shown during the presentation. One of these is the Crab Nebula shown in Fig 3 and its immediate surroundings. This region was chosen for several reasons including the fact that it is a standard candle for many γ-ray observatories including HAWC, the extensive dedicated

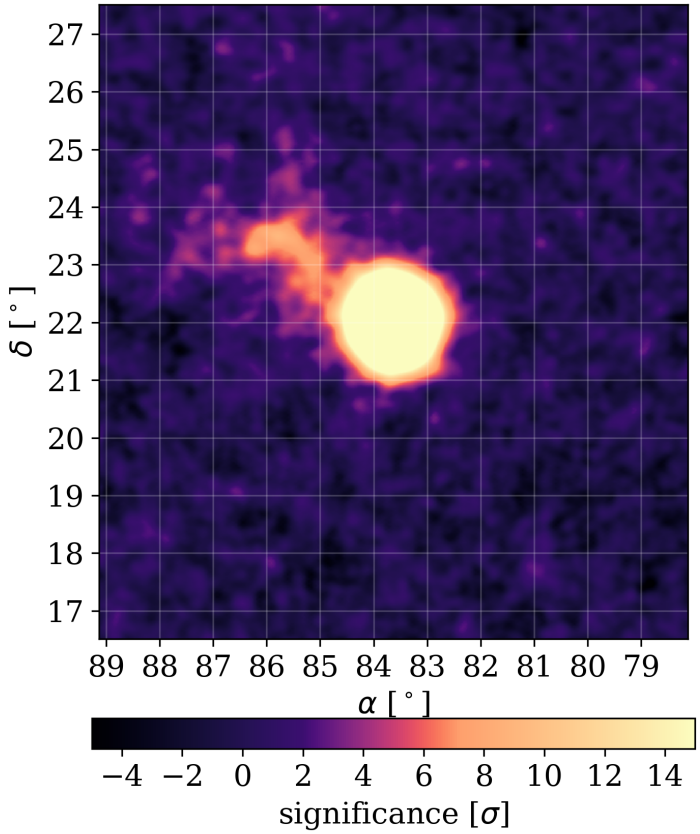

Figure 3: View of the Crab Nebula and surrounding region from 78° to 90° RA and 16° to 28° Declination

analyses done over the years in HAWC data [4] and [5], and the relative isolation from the diffuse emission near the galactic plane. Results from the fit will be shown. The second region studied as a benchmark was the Cygnus Cocoon region which can be seen near 80° in Fig 1. This was chosen for several reasons such as the complexity of the region which caused previous catalog methods to miss source components, the presence of mild diffuse background emission in the region, and the fact that a recent dedicated analysis of the region provides good results to compare with [6]. This fit will also be shown on the poster. While the region in Fig 1 is much less complicated and overlapping than Fig 2 we hope that the method will perform equally well at disentangling soures in the region and provide much better results than the previously used methods.

2.1 Acknowledgements

We acknowledge the support from: the US National Science Foundation (NSF); the US Department of Energy Office of High-Energy Physics; the Laboratory Directed Research and Development (LDRD) program of Los Alamos National Laboratory; Consejo Nacional de Ciencia y Tecnología

(CONACyT), México, grants 271051, 232656, 260378, 179588, 254964, 258865, 243290, 132197, A1-S-46288, A1-S-22784, CF-2023-I-645, cátedras 873, 1563, 341, 323, Red HAWC, México; DGAPA-UNAM grants IG101323, IN111716-3, IN111419, IA102019, IN106521, IN110621, IN110521 , IN102223; VIEP-BUAP; PIFI 2012, 2013, PROFOCIE 2014, 2015; the University of Wisconsin Alumni Research Foundation; the Institute of Geophysics, Planetary Physics, and Signatures at Los Alamos National Laboratory; Polish Science Centre grant, DEC-2017/27/B/ST9/02272; Coordinación de la Investigación Científica de la Universidad Michoacana; Royal Society - Newton Advanced Fellowship 180385; Generalitat Valenciana, grant CIDEGENT/2018/034; The Program Management Unit for Human Resources & Institutional Development, Research and Innovation, NXPO (grant number B16F630069); Coordinación General Académica e Innovación (CGAI-UdeG), PRODEP-SEP UDG-CA-499; Institute of Cosmic Ray Research (ICRR), University of Tokyo. H.F. acknowledges support by NASA under award number 80GSFC21M0002. We also acknowledge the significant contributions over many years of Stefan Westerhoff, Gaurang Yodh and Arnulfo Zepeda Dominguez, all deceased members of the HAWC collaboration. Thanks to Scott Delay, Luciano Díaz and Eduardo Murrieta for technical support.

References

[1] M. Ackermann *et al.*, "Search for extended sources in the galactic plane using six years of fermi-large area telescope pass 8 data above 10 GeV," *The Astrophysical Journal*, vol. 843, no. 2, p. 139, Jul. 2017. DOI: 10.3847/1538-4357/aa775a. [Online]. Available: https://doi.org/10.3847%5C%2F1538-4357%5C%2Faa775a.

[2] P. W. Younk *et al.*, *A high-level analysis framework for hawc*, 2015. arXiv: 1508.07479 [astro-ph.IM].

[3] S. S. Wilks, "The large-sample distribution of the likelihood ratio for testing composite hypotheses," *The Annals of Mathematical Statistics*, vol. 9, no. 1, pp. 60–62, 1938, ISSN: 00034851. [Online]. Available: http://www.jstor.org/stable/2957648 (visited on 06/26/2023).

[4] A. U. Abeysekara *et al.*, "Measurement of the crab nebula spectrum past 100 TeV with HAWC," *The Astrophysical Journal*, vol. 881, no. 2, p. 134, Aug. 2019. DOI: 10.3847/1538-4357/ab2f7d. [Online]. Available: https://doi.org/10.3847%2F1538-4357%2Fab2f7d.

[5] A. U. Abeysekara *et al.*, "Observation of the crab nebula with the HAWC gamma-ray observatory," *The Astrophysical Journal*, vol. 843, no. 1, p. 39, Jun. 2017. DOI: 10.3847/1538-4357/aa7555. [Online]. Available: https://doi.org/10.3847%2F1538-4357%2Faa7555.

[6] A. U. Abeysekara *et al.*, "HAWC observations of the acceleration of very-high-energy cosmic rays in the cygnus cocoon," *Nature Astronomy*, vol. 5, no. 5, pp. 465–471, Mar. 2021. DOI: 10.1038/s41550-021-01318-y. [Online]. Available: https://doi.org/10.1038%2Fs41550-021-01318-y.

Full Authors List: HAWC Collaboration

A. Albert[1], R. Alfaro[2], C. Alvarez[3], A. Andrés[4], J.C. Arteaga-Velázquez[5], D. Avila Rojas[2], H.A. Ayala Solares[6], R. Babu[7], E. Belmont-Moreno[2], T. Capistrán[4], Y. Cárcamo[26], A. Carramiñana[9], F. Carreón[4], U. Cotti[5], J. Cotzomi[26], S. Coutiño de León[10], E. De la Fuente[11], D. Depaoli[12], C. de León[5], R. Diaz Hernandez[9], J.C. Díaz-Vélez[11], B.L. Dingus[1], M. Durocher[1], M.A. DuVernois[10], K. Engel[8], C. Espinoza[2], K.L. Fan[8], K. Fang[10], N.I. Fraija[4], J.A. García-González[13], F. Garfias[4], H. Goksu[12], M.M. González[4], J.A. Goodman[8], S. Groetsch[7], J.P. Harding[1], S. Hernandez[2], I. Herzog[14], J. Hinton[12], D. Huang[7], F. Hueyotl-Zahuantitla[3], P. Hüntemeyer[7], A. Iriarte[4], V. Joshi[28], S. Kaufmann[15], D. Kieda[16], A. Lara[17], J. Lee[18], W.H. Lee[4], H. León Vargas[2], J. Linnemann[14], A.L. Longinotti[4], G. Luis-Raya[15], K. Malone[19], J. Martínez-Castro[20], J.A.J. Matthews[21], P. Miranda-Romagnoli[22], J. Montes[4], J.A. Morales-Soto[5], M. Mostafá[6], L. Nellen[23], M.U. Nisa[14], R. Noriega-Papaqui[22], L. Olivera-Nieto[12], N. Omodei[24], Y. Pérez Araujo[4], E.G. Pérez-Pérez[15], A. Pratts[2], C.D. Rho[25], D. Rosa-Gonzalez[9], E. Ruiz-Velasco[12], H. Salazar[26], D. Salazar-Gallegos[14], A. Sandoval[2], M. Schneider[8], G. Schwefer[12], J. Serna-Franco[2], A.J. Smith[8], Y. Son[18], R.W. Springer[16], O. Tibolla[15], K. Tollefson[14], I. Torres[9], R. Torres-Escobedo[27], R. Turner[7], F. Ureña-Mena[9], E. Varela[26], L. Villaseñor[26], X. Wang[7], I.J. Watson[18], F. Werner[12], K. Whitaker[6], E. Willox[8], H. Wu[10], H. Zhou[27]

[1]Physics Division, Los Alamos National Laboratory, Los Alamos, NM, USA, [2]Instituto de Física, Universidad Nacional Autónoma de México, Ciudad de México, México, [3]FCFM-MCTP, Universidad Autónoma de Chiapas, Tuxtla Gutiérrez, Chiapas, México, [4]Instituto de Astronomía, Universidad Nacional Autónoma de México, Ciudad de México, México, [5]Instituto de Física y Matemáticas, Universidad Michoacana de San Nicolás de Hidalgo, Morelia, Michoacán, México, [6]Department of Physics, Pennsylvania State University, University Park, PA, USA, [7]Department of Physics, Michigan Technological University, Houghton, MI, USA, [8]Department of Physics, University of Maryland, College Park, MD, USA, [9]Instituto Nacional de Astrofísica, Óptica y Electrónica, Tonantzintla, Puebla, México, [10]Department of Physics, University of Wisconsin-Madison, Madison, WI, USA, [11]CUCEI, CUCEA, Universidad de Guadalajara, Guadalajara, Jalisco, México, [12]Max-Planck Institute for Nuclear Physics, Heidelberg, Germany, [13]Tecnologico de Monterrey, Escuela de Ingeniería y Ciencias, Ave. Eugenio Garza Sada 2501, Monterrey, N.L., 64849, México, [14]Department of Physics and Astronomy, Michigan State University, East Lansing, MI, USA, [15]Universidad Politécnica de Pachuca, Pachuca, Hgo, México, [16]Department of Physics and Astronomy, University of Utah, Salt Lake City, UT, USA, [17]Instituto de Geofísica, Universidad Nacional Autónoma de México, Ciudad de México, México, [18]University of Seoul, Seoul, Rep. of Korea, [19]Space Science and Applications Group, Los Alamos National Laboratory, Los Alamos, NM USA [20]Centro de Investigación en Computación, Instituto Politécnico Nacional, Ciudad de México, México, [21]Department of Physics and Astronomy, University of New Mexico, Albuquerque, NM, USA, [22]Universidad Autónoma del Estado de Hidalgo, Pachuca, Hgo., México, [23]Instituto de Ciencias Nucleares, Universidad Nacional Autónoma de México, Ciudad de México, México, [24]Stanford University, Stanford, CA, USA, [25]Department of Physics, Sungkyunkwan University, Suwon, South Korea, [26]Facultad de Ciencias Físico Matemáticas, Benemérita Universidad Autónoma de Puebla, Puebla, México, [27]Tsung-Dao Lee Institute and School of Physics and Astronomy, Shanghai Jiao Tong University, Shanghai, China, [28]Erlangen Centre for Astroparticle Physics, Friedrich Alexander Universität, Erlangen, BY, Germany

PoS(ICRC2023)759